jove

Visualizing the DNA Damage Response in Purkinje Cells Using Cerebellar Organotypic Cultures

Sharone Naor[1], **Yael Ziv**[1], **Yosef Shiloh**[1]

[1] The David and Inez Myers Laboratory for Cancer Genetics, Department of Human Molecular Genetics and Biochemistry, Faculty of Health and Medical Sciences, School of Medicine, Tel Aviv University

Corresponding Author

Yosef Shiloh
yossih@tauex.tau.ac.il

Citation

Naor, S., Ziv, Y., Shiloh, Y. Visualizing the DNA Damage Response in Purkinje Cells Using Cerebellar Organotypic Cultures. *J. Vis. Exp.* (214), e67167, doi:10.3791/67167 (2024).

Date Published

December 27, 2024

DOI

10.3791/67167

URL

jove.com/video/67167

Abstract

Cerebellar Purkinje cells (PCs) exhibit a unique interplay of high metabolic rates, specific chromatin architecture, and extensive transcriptional activity, making them particularly vulnerable to DNA damage. This necessitates an efficient DNA damage response (DDR) to prevent cerebellar degeneration, often initiated by PC dysfunction or loss. A notable example is the genome instability syndrome, ataxia-telangiectasia (A-T), marked by progressive PC depletion and cerebellar deterioration. Investigating DDR mechanisms in PCs is vital for elucidating the pathways leading to their degeneration in such disorders. However, the complexity of isolating and cultivating PCs *in vitro* has long hindered research efforts. Murine cerebellar organotypic (slice) cultures offer a feasible alternative, closely mimicking the *in vivo* tissue environment. Yet, this model is constrained to DDR indicators amenable to microscopic imaging. We have refined the organotypic culture protocol, demonstrating that fluorescent imaging of protein-bound poly(ADP-ribose) (PAR) chains, a rapid and early DDR indicator, effectively reveals DDR dynamics in PCs within these cultures, in response to genotoxic stress.

Introduction

The integrity of cellular DNA is constantly under threat from DNA damaging agents, predominantly metabolic by-products like reactive oxygen species, which inflict tens of thousands of DNA lesions per cell daily[1]. The persistent upkeep of genome stability is essential for cellular homeostasis[2,3]. The cornerstone of this maintenance is the DNA damage response (DDR) - an intricate, layered signaling network that initiates specific DNA repair pathways while carefully adjusting many other cellular processes[4,5]. Deficits in the DDR are commonly manifested as 'genome instability syndromes,' marked by chromosomal instability, progressive tissue deterioration, impaired growth or development, a predisposition to cancer, and heightened sensitivity to particular DNA-damaging agents[6,7,8,9]. Notably, neurodegeneration, which often

includes cerebellar atrophy, is a distinct feature of many genome instability syndromes[7,10,11,12].

The autosomal recessive disorder, ataxia-telangiectasia (A-T), is a well-documented example of a genome instability disorder[13,14,15]. This condition arises from null mutations in the *ATM* (A-T, mutated) gene, responsible for coding the pivotal protein kinase, ATM, which is known primarily as a DDR mobilizer in response to DNA double-strand breaks (DSBs)[16,17]. A-T manifests as a multisystem disorder, predominantly characterized by progressive cerebellar degeneration, leading to acute motor impairments, immunodeficiency, gonadal atrophy, cancer predisposition, and extreme sensitivity to ionizing radiation. Cultured cells from individuals with A-T show chromosomal instability and increased sensitivity to genotoxic agents, especially those causing DSBs[15,18,19]. Importantly, ATM also plays a role in repairing other DNA lesions, underscoring its broad significance in maintaining genome stability[20,21,22].

Despite thorough research into ATM's numerous roles, the specific mechanism leading to cerebellar degeneration in A-T remains a topic of active debate, with various models proposed to elucidate this process[23,24,25,26,27,28,29,30]. Our model[28] suggests that cerebellar degeneration in A-T patients begins with the dysfunction and eventual loss of Purkinje cells (PCs). Considering ATM's critical role in preserving genome stability in the face of ongoing DNA damage, PCs are particularly vulnerable to the absence of ATM. We attribute this vulnerability to the combination of their high metabolic activity, distinctive chromatin structure, and extensive transcriptional activity. Ultimately, it is suggested that the loss of PC function, and hence, their degeneration, is due to the stochastic, functional inactivation of genes, a consequence of producing defective transcripts[28].

The study of PC biology in the laboratory is impeded by challenges in cultivating isolated PCs, as these cells rely heavily on their natural milieu and neighboring cells for survival and function, rendering them incompatible with dissociated culture growth. Nonetheless, PCs can remain viable for extended periods in tissue slice cultures. Cerebellar organotypic cultures, which are tissue slices typically derived from rodent cerebella, maintain the tissue's structural organization and support various experimental manipulations analogous to those possible with cultured cells. Therefore, these cultures allow for cerebellar studies within a controlled setting[31,32,33,34,35,36,37,38,39,40,41,42,43]. Specifically, in the context of A-T, murine cerebellar organotypic cultures have proven to be instrumental in exploring the DDR in Atm-deficient PCs[40,41,42,43]. While Atm-deficient mice display only a subtle cerebellar phenotype[44,45,46,47], presumably due to differences between human and mouse cerebellar physiology, the assumption is that ATM's roles are largely conserved across these species. This notion is supported by our observations that the deficient response to DNA DSBs in *Atm*$^{-/-}$ murine PCs aligns with that observed in other murine and human ATM/Atm-deficient cell types[40,41,42,43].

A limitation in analyzing PC responses to various stimuli or stresses within organotypic cultures is the necessity to rely on microscopic imaging for readouts. The DDR is usually studied using bulk biochemical readouts, although common immunofluorescent markers are utilized as well, such as following the dynamics of formation and resolution of nuclear foci of phosphorylated histone H2AX (γH2AX) and the 53BP1 protein, which are considered indicators of DSBs[48,49]. A broader measure is the fluorescent imaging of poly(ADP-

ribose) (PAR) chain formation on proteins, a rapid and robust early DNA damage response, particularly to strand breaks[7,50]. We modified the protocol by Komulainen et al.[51] for PAR staining in cerebellar organotypic cultures. We observed a pronounced PAR response in the sizeable nuclei of PCs. Presented here is our refined protocol for establishing murine cerebellar organotypic cultures and for visualizing the PAR response under genotoxic stress.

Protocol

See **Table of Materials** for details of materials, equipment, and antibodies. Animal procedures were employed under the ethical guidelines of Tel Aviv University's Ethics Committee after approval. The procedure is carried out on 10-day old mouse pups, regardless of their sex. If needed, genotyping is performed on the previous day using a tail biopsy and standard methods. Solutions are sterile and stored at 4 °C unless indicated otherwise; see **Table 1**.

1. Preparation of cultures

NOTE: Conduct the procedure within a sterile environment and disinfect the work surface in advance using 70% ethanol.

1. Add 1 mL of BME to each well of 6-well plates. Using sterile forceps, place a single cell culture insert into each well and incubate the plates in a 37 °C/5% CO_2 incubator for a minimum of 2 h prior to the dissection procedure.
2. Set up a dissection area within a biological hood, containing the tissue chopper, 30 mm culture plates, a binocular microscope, and a light source.
3. Immerse the surgical tools in 70% ethanol throughout the process. Use a urinary cup filled with 70% ethanol for immersion, and a separate urinary cup with 1x PBS to wash off the ethanol before use.
4. For each dissection (i.e., for each cerebellum), prepare two 30 mm culture plates filled with cold dissection medium and leave them on ice.
5. Spray the animal with 70% ethanol.
6. Using sharp scissors, swiftly decapitate the animal. To expose the brain, make a small incision with scissors away from the cerebellum. Using tweezers with rounded ends, gently peel off the skull. Remove the skull in small pieces to avoid damaging the cerebellar tissue.
7. Immediately transfer the brain into cold dissection medium or directly remove the cerebellum from within the skull. To do this, expose the cerebellum and separate the cerebellar cortex from the brainstem by disconnecting the three pairs of peduncles, using a fine curved iris spatula. To identify the peduncles, view from rostral to caudal: the paired superior cerebellar peduncles connect the midbrain to each side of the cerebellum; the paired middle cerebellar peduncles connect the pons to each side of the cerebellum; and the paired inferior cerebellar peduncles connect to the medulla to each side of to the cerebellum. Once the cerebellum is visible, separate it from the cerebrum using the same spatula: slide the spatula between the cerebellum, the superior colliculus, and the brainstem.
   NOTE: Do not make a special effort to remove the meninges as they readily detach after the cerebellum is sliced.
8. Set the tissue chopper to a slice thickness of 350 µm.
9. Prior to positioning the cerebellum on the chopper's base, remove excess dissecting buffer from the tissue. This will improve the tissue's adhesion to the chopper's base.
10. Position the cerebellum on the cutting platform in a vertical orientation and carry out parasagittal slicing at

a slice thickness of 350 µm. Gently separate the slices using a fine iris spatula and put them into cold dissection medium.

11. Transfer the sliced tissue back to a fresh cold dissection buffer. Use a 1,000 µL tip to delicately guide the tissue slices into the dish containing cold dissection buffer.

12. Under the binocular use two curved iris spatulas to carefully separate the tissue slices from each other. For cultures, use slices derived from the cerebellar vermis situated in the medial cortico-nuclear zone of the organ.

13. Transfer each tissue slice onto a culture insert using a wide spatula and move each insert carrying a tissue slice into a well in the 6-well plates containing the pre-warmed medium. Leave the plates in the incubator.

14. Replace the medium every other day: aspirate the used medium using a sterile glass pipette, and with a 5 mL serological pipette, add 1 mL of fresh MBE with the pipette's tip leaning against the well's wall. Make sure not to direct the medium flow onto the tissue.
    NOTE: The tissue slice will exhibit an inflammation-like appearance for the first 5-7 days in culture and will be ready for experiments as soon as this phenomenon disappears and up to 2 weeks after culture establishment.

2. Treatment with DNA damaging agents, fixation, staining, and microscopic imaging

1. Add DNA-damaging chemicals directly to the culture medium at appropriate final concentrations, for predetermined durations. After the exposure period, remove the chemicals by replacing the medium with fresh culture medium.

2. If the DDR readout involves PAR staining, add an inhibitor of poly(ADP-ribose) glycohydrolase (PARG) to the culture medium at a final concentration of 10 µM, 30 min prior to fixation.
    NOTE: This treatment is critical as the PAR modification is short-lived and continuously degraded by PARG.

3. Immediately prior to fixation, aspirate the medium and replace it with 1 mL of 0.1 M phosphate buffer at room temperature.
    NOTE: Cold buffer might cause detachment of the tissue slices from the insert.

4. Immediately fix the slices by replacing the buffer with precooled (-20 °C) acetone:methanol mix (1:1) such that the tissue slice is submerged in this mix and leave for 20 min at -20 °C.
    NOTE: It is possible to stop at this stage and proceed with immunostaining later. To do so, wash the tissues 3x with 0.1 M phosphate buffer precooled to 4 °C, making sure the tissue is submerged in the buffer. Tissues can be stored now in 0.1M phosphate buffer for up to 2 weeks at 4 °C.

5. Transfer the tissue slice into a well in a 48-well plate.

6. Use a scalpel and a cutting board to remove the margins of the insert, cutting around the tissue slice. Place each slice in a well of a 48-well plate. Add 100 µL of 0.1 M phosphate buffer.

7. For permeabilization, aspirate the buffer, add to the well 100 µL of 0.1 M phosphate buffer containing 1% Triton X-100, and leave for 5 min at room temperature.

8. Aspirate the solution and add 100 µL of blocking solution (see **Table 1**) per well. Shake gently at room temperature for 2 h.

9. During the blocking step, dilute the primary antibody or anti-PAR reagent (1:800) in the blocking solution.
10. Remove the blocking solution (no need to wash) and add 100 µL of primary antibody mix to each well. Apply gentle shaking for 2 h at room temperature.
11. Dilute the secondary antibodies in 0.1 M phosphate buffer containing 0.2% Triton X-100 (1:500) while minimizing their exposure to light.
12. Aspirate the primary antibody solution and wash the slices 3 x 5 min with 0.1 M phosphate buffer containing 0.2% Triton X-100, at room temperature, with gentle shaking.
13. Replace the wash solution with 100 µL of secondary antibody solution (1:500 dilution). Continue gentle shaking for 2 h at room temperature in the dark (cover the plates with aluminum foil).
14. To prepare a DAPI solution, dilute the stock solution (2 mg/mL) to 1 µg/mL in 1x PBS.
15. Twenty minutes before the end of the 2 h incubation with the secondary antibody, add 20 µL of the final DAPI solution to each well and continue shaking for 20 min. Aspirate the liquid and wash with the wash solution for 3 x 5 min with gentle shaking.
16. For mounting, place the tissue on a microscope glass slide with the tissue facing up, add mounting medium, and cover with a cover glass. Place the slides on a flat surface and let them dry overnight in the dark, at room temperature (avoid using mounting medium containing DAPI to prevent blurriness).
17. Store the slides at 4 °C in a lightproof box.
18. Capture microscopic images using a confocal microscope and appropriate filters.

Representative Results

Figure 1 illustrates the general appearance of the cerebellar organotypic cultures. The top row in **Figure 1A** shows the cerebellar foliation, which is maintained in culture, while the bottom row shows the PCs stained for Calbindin D-28k (green) and the neuronal nuclei stained for NeuN (red). In **Figure 1B**, the astrocytes in the PCs (red) are stained for GFAP (green), an intermediate filament type III protein. **Figure 2** and **Figure 3** show the PAR staining observed after treating these cultures with two DNA-damaging agents, both of which are strong oxidants: potassium bromate (a final concentration of 10 mM for 12 h) and paraquat. The PAR response was marked in the treated PCs in the cerebellar folium compared to the control.

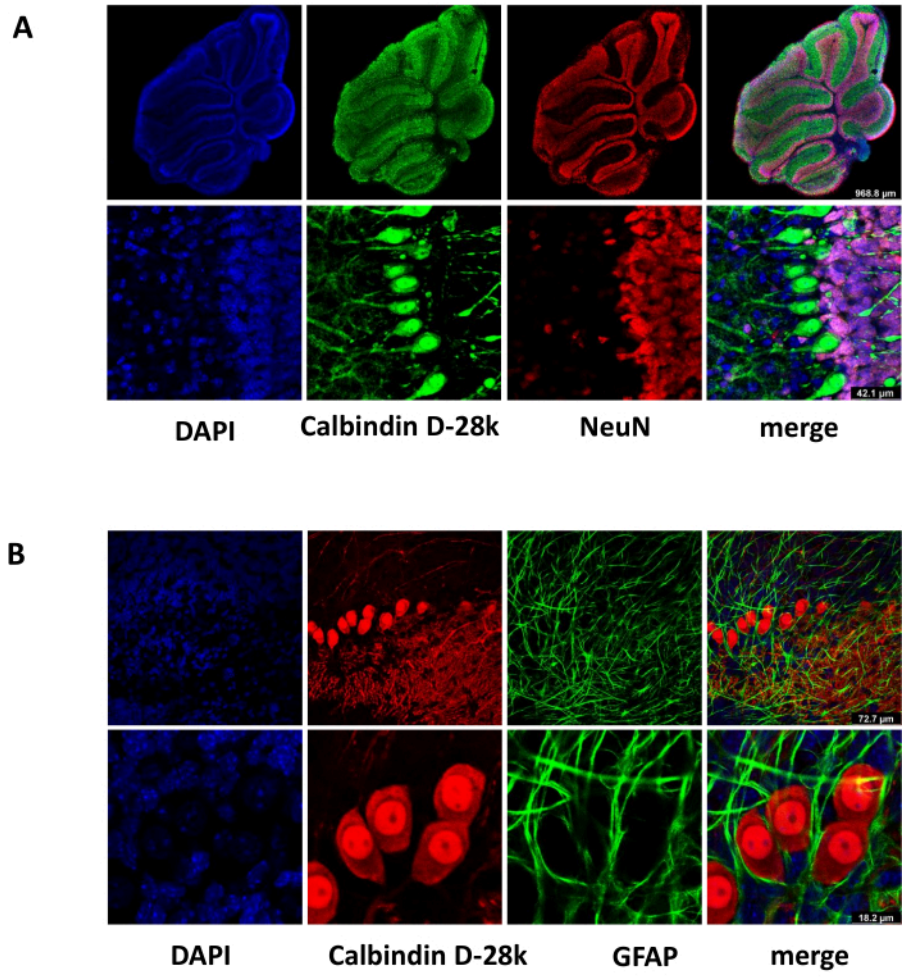

Figure 1: Overview of murine cerebellar organotypic cultures. (**A**) The top row illustrates the cerebellar foliation, which is maintained in culture. The bottom row focuses on the PC layer. PCs are highlighted by Calbindin D-28k (green). NeuN staining (red) identifies neuronal nuclei across the layers. (**B**) A closer look at PCs (red). GFAP (green), an intermediate filament type III protein, which highlights astrocytes. Scale bars = 968.8 µm (**A**, top row), 42.1 µm (**A**, second row), 72.7 µm (**B**, top row), 18.2 µm (**B**, second row). Abbreviations: PC = Purkinje cells; GFAP = glial fibrillary acidic protein; DAPI = 4',6-diamidino-2-phenylindole. Please click here to view a larger version of this figure.

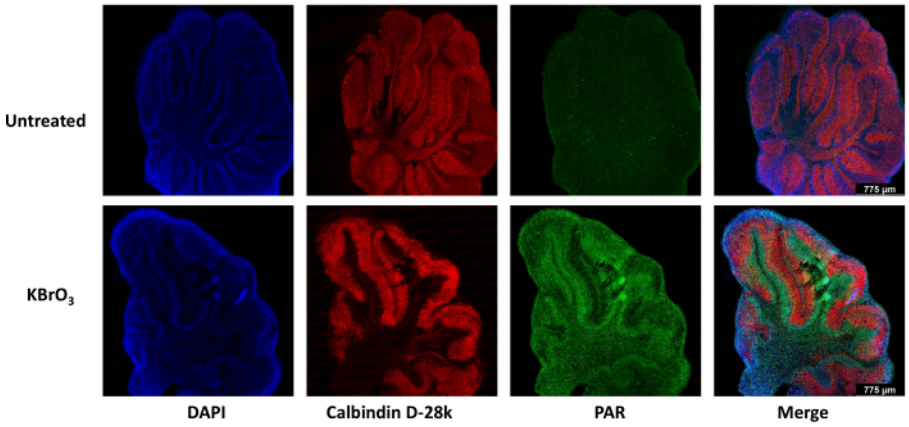

Figure 2: PAR staining in a cerebellar slice treated with potassium bromate. The cerebellar slice was treated with potassium bromate ($KBrO_3$)-a potent oxidizing agent, at a final concentration of 10 mM for 12 h. Scale bars = 775 µm. Abbreviations: PAR = poly(ADP-ribose); DAPI = 4',6-diamidino-2-phenylindole. Please click here to view a larger version of this figure.

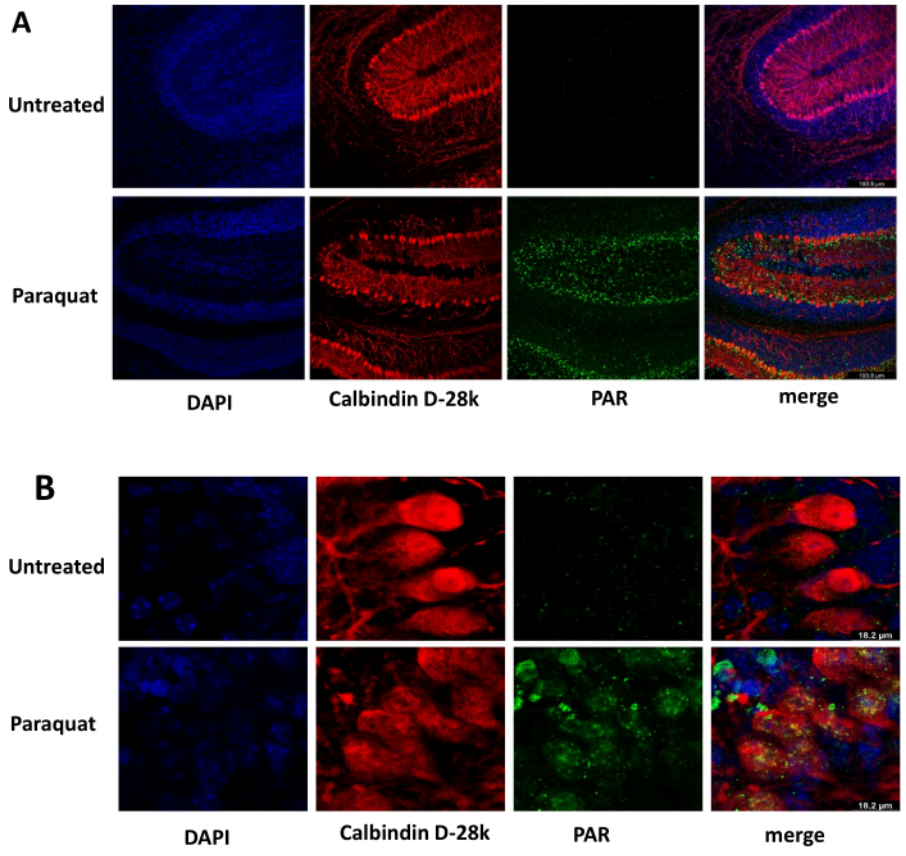

Figure 3: PAR response in cerebellar slices exposed to paraquat, a strong producer of superoxide anions. (**A**) A general view of a cerebellar folium. Note the robust PAR response particularly in PCs compare to the control. (**B**) A closer examination shows the PAR response in PCs and other cell types. Scale bars = 193.8 µm (**A**), 18.2 µm (**B**). Abbreviations: PAR = poly(ADP-ribose); DAPI = 4',6-diamidino-2-phenylindole. Please click here to view a larger version of this figure.

Solutions and buffers	
Solution	**Ingredients**
Dissection medium	Hank's balanced salt solution (HBSS) containing 0.5% D-glucose. Add 0.5 mL of 50% D-glucose solution to 50 mL of HBSS without Mg^{2+} and Ca^{2+}.
BME culture medium	Mix 100 mL of Basal Medium Eagle (BME) containing phenol red but not L-glutamine or HEPES, with 50 mL of HBSS with phenol red, 50 mL of heat-inactivated horse serum, 2 mL of 50% D-glucose, and 1 mL of 200 mM L-glutamine. Mix and filter through a 0.22 µm filter in a sterile environment. Store at 4 °C
Blocking solution for immunostaining	in 0.1 M Phosphate buffer: add 0.5% Triton X-100, 10% Goat serum
Secondary antibody dilution buffer	0.1 M phosphate buffer, 0.2%Triton X-100
Wash buffer	0.1 M phosphate buffer, 0.2%Triton X-100
Fixative solution	Actenoe:methanol (1:1 v:v)
Permeabilization solution	0.1 M phosphate buffer, 1%Triton X-100
DAPI solution	Stock solution (2 mg/mL) diluted to 1 µg/mL in 1x PBS
Phosphate Buffer	Prepare two soulutions A and B (see below). Mix solutions according to the ratios specified below to make 0.2 M phosphate buffer. Then dilute the 0.2M solution with DDW (1:1) to make 0.1 M phosphate buffer (working solution).
solution A (for 0.2 M)	12 g of Sodium Phosphate Monobasic Anhydrous (Na_2HPO_4 FW 141.96) 500 mL of DDW
Solution B (for 0.2 M)	14.2 g of Sodium phosphate diabasic anhydrous (Na_2HPO_4 FW 141.96) 500 mL of DDW
Mixed solutions to make 0.2 M	Prepare 1 L: 230 mL of solution A and 770 mL of solution B
0.1 M phosphate buffer	Dilute the mixed solution with DDW (1:1)

Table 1: Solutions and their composition.

Discussion

General comments

The major advantage of the organotypic culture system is that it facilitates studies using the cerebellar cortex tissue, preserving its structural organization for several weeks in the culture dish setup. This system is useful for conducting in-depth morphological analyses of Purkinje cells (PCs), including detailed examinations of dendritic spines and ultrastructural features[52,53,54,55,56,57,58,59]. Our observations indicate that the DNA damage response (DDR) is notably active in PCs within these cultures. However, the major limitations of this system include the limited duration of its use and its reliance on microscopic imaging to monitor cellular processes, highlighting the ongoing need to develop or adapt suitable imaging techniques.

Another word of caution pertains to the cerebellar portion that is dissected for preparing the tissue slices. We have observed that different cerebellar lobes can yield cultures with markedly different internal organization and overall quality. Therefore, we prefer to establish cultures from slices obtained via midsagittal sections of the cerebellar vermis. In these slices, the folia of the cerebellar cortex are conveniently visible.

It is advisable to utilize tissue slices obtained from the cerebellar vermis, which exhibit the characteristic foliation of the cerebellar cortex. These slices maintain their organizational structure in culture for several weeks. Furthermore, it is recommended to commence experimental procedures with the cultures approximately 7-12 days post establishment. A typical experiment designed to assess the DNA damage response in these cultures involves initiating damage by irradiation or by the addition of DNA-damaging chemicals to the culture medium. Subsequently, tissue fixation and staining are performed at various time intervals. To assess recovery from chemical-induced damage, a period of incubation in fresh medium is included. It is advisable to initiate long-term experiments at the earliest opportunity, ideally around 7 days following culture establishment.

The cerebellar organotypic cultures are maintained in a medium devoid of antibiotics; thus, maintaining a sterile environment during their establishment is imperative. The age of the pups from which the cerebella are harvested is critical, with a recommended range of 9-12 days. This age range is optimal as the cerebellar cortex is sufficiently developed for sectioning. Notably, in older animals, the tissues tend to adhere to the blade. It is crucial to keep the cerebellum immersed in a cold dissection solution until dissected.

During the initial 5-7 days in culture, the tissue slices may exhibit signs reminiscent of inflammation, characterized by swelling and milky discoloration. These attributes can potentially affect the measurement of physiological parameters and the effectiveness of immunostaining techniques.

It is highly recommended not to slice the cerebellum thinner than 350 µm to avoid inconsistency in thickness during slicing. Keep in mind that a 350 µm-slice tissue gets much thinner after 7 days in culture to around 90 µm (based on Z stack measurement).

Here, we introduce PAR staining[7,50] to the toolkit used to investigate the DDR in PCs. This readout is rapid, sensitive, and captures the dynamic nature of the DDR, proving especially useful in our analysis of the DDR in wild-type and Atm-deficient PCs. The protocols outlined here should be particularly beneficial for researchers studying genomic instability syndromes that affect the cerebellum.

Disclosures

The authors declare no conflicts of interest related to this study.

Acknowledgments

Work in our lab is supported by the Dr. Miriam and Sheldon G. Adelson Medical Research Foundation and the Israeli Association for Fighting the A-T Disease.

References

1. Tubbs, A. Nussenzweig, A. Endogenous DNA damage as a source of genomic instability in cancer. *Cell.* **168** (4), 644-656 (2017).
2. Negrini, S., Gorgoulis, V. G., Halazonetis, T. D. Genomic instability--an evolving hallmark of cancer. *Nat Rev Mol Cell Biol.* **11** (3), 220-228 (2010).
3. De Almeida, L. C., Calil, F. A., Machado-Neto, J. A., Costa-Lotufo, L. V. DNA damaging agents and DNA repair: From carcinogenesis to cancer therapy. *Cancer Genet.* **252-253,** 6-24 (2021).
4. Sirbu, B. M. Cortez, D. DNA damage response: Three levels of DNA repair regulation. *Cold Spring Harb Perspect Biol.* **5** (8), a012724 (2013).
5. Chatterjee, N. Walker, G. C. Mechanisms of DNA damage, repair, and mutagenesis. *Environ Mol Mutagen.* **58** (5), 235-263 (2017).
6. Taylor, A. M. R. et al. Chromosome instability syndromes. *Nat Rev Dis Primers.* **5** (1), 64 (2019).
7. Caldecott, K. W. DNA single-strand break repair and human genetic disease. *Trends Cell Biol.* **32** (9), 733-745 (2022).
8. Tiwari, V. Wilson, D. M., 3rd. DNA damage and associated DNA repair defects in disease and premature aging. *Am J Hum Genet.* **105** (2), 237-257 (2019).
9. Rieckher, M., Garinis, G. A., Schumacher, B. Molecular pathology of rare progeroid diseases. *Trends Mol Med.* **27** (9), 907-922 (2021).
10. Qing, X., Zhang, G., Wang, Z. Q. DNA damage response in neurodevelopment and neuromaintenance. *FEBS J.* **290** (13), 3300-3310 (2023).
11. Scheijen, E. E. M. Wilson, D. M., 3rd. Genome integrity and neurological disease. *Int J Mol Sci.* **23** (8), (2022).
12. Welch, G. Tsai, L. H. Mechanisms of DNA damage-mediated neurotoxicity in neurodegenerative disease. *EMBO Rep.* **23** (6), e54217 (2022).
13. Perlman, S. L., Boder Deceased, E., Sedgewick, R. P., Gatti, R. A. Ataxia-telangiectasia. *Handb Clin Neurol.* **103**, 307-332 (2012).
14. Rothblum-Oviatt, C. et al. Ataxia telangiectasia: A review. *Orphanet J Rare Dis.* **11** (1), 159 (2016).
15. Amirifar, P., Ranjouri, M. R., Yazdani, R., Abolhassani, H., Aghamohammadi, A. Ataxia-telangiectasia: A review of clinical features and molecular pathology. *Pediatr Allergy Immunol.* **30** (3), 277-288 (2019).
16. Shiloh, Y. Ziv, Y. The atm protein kinase: Regulating the cellular response to genotoxic stress, and more. *Nat Rev Mol Cell Biol.* **14** (4), 197-210 (2013).
17. Lee, J. H. Paull, T. T. Cellular functions of the protein kinase atm and their relevance to human disease. *Nat Rev Mol Cell Biol.* **22** (12), 796-814 (2021).
18. Taylor, A. M. et al. Ataxia telangiectasia: A human mutation with abnormal radiation sensitivity. *Nature.* **258** (5534), 427-429 (1975).

19. Shiloh, Y., Tabor, E., Becker, Y. Cellular hypersensitivity to neocarzinostatin in ataxia-telangiectasia skin fibroblasts. *Cancer Res.* **42** (6), 2247-2249 (1982).
20. Shiloh, Y. Atm: Expanding roles as a chief guardian of genome stability. *Exp Cell Res.* **329** (1), 154-161 (2014).
21. Shiloh, Y. Lederman, H. M. Ataxia-telangiectasia (a-t): An emerging dimension of premature ageing. *Ageing Res Rev.* **33**, 76-88 (2017).
22. Geng, A. et al. Sirt2 promotes base excision repair by transcriptionally activating ogg1 in an atm/atr-dependent manner. *Nucleic Acids Res.* **52** (9), 5107-5120 (2024).
23. Biton, S., Barzilai, A., Shiloh, Y. The neurological phenotype of ataxia-telangiectasia: Solving a persistent puzzle. *DNA Repair (Amst).* **7** (7), 1028-1038 (2008).
24. Kanner, S. et al. Astrocytes restore connectivity and synchronization in dysfunctional cerebellar networks. *Proc Natl Acad Sci U S A.* **115** (31), 8025-8030 (2018).
25. Song, X., Ma, F., Herrup, K. Accumulation of cytoplasmic DNA due to atm deficiency activates the microglial viral response system with neurotoxic consequences. *J Neurosci.* **39** (32), 6378-6394 (2019).
26. Levi, H. et al. Dysfunction of cerebellar microglia in ataxia-telangiectasia. *Glia.* **70** (3), 536-557 (2022).
27. Bourseguin, J. et al. Persistent DNA damage associated with atm kinase deficiency promotes microglial dysfunction. *Nucleic Acids Res.* **50** (5), 2700-2718 (2022).
28. Shiloh, Y. The cerebellar degeneration in ataxia-telangiectasia: A case for genome instability. *DNA Repair (Amst).* **95**, 102950 (2020).
29. Lai, J. et al. Atm-deficiency-induced microglial activation promotes neurodegeneration in ataxia-telangiectasia. *Cell Rep.* **43** (1), 113622 (2024).
30. Woolley, P. R. et al. Regulation of transcription patterns, poly(adp-ribose), and rna-DNA hybrids by the atm protein kinase. *Cell Rep.* **43** (3), 113896 (2024).
31. Santos, G., Barateiro, A., Brites, D., Fernandes, A. S100b impairs oligodendrogenesis and myelin repair following demyelination through rage engagement. *Front Cell Neurosci.* **14**, 279 (2020).
32. Iskusnykh, I. Y., Fattakhov, N., Buddington, R. K., Chizhikov, V. V. Intrauterine growth restriction compromises cerebellar development by affecting radial migration of granule cells via the jamc/pard3a molecular pathway. *Exp Neurol.* **336**, 113537 (2021).
33. Gehmeyr, J. et al. Disabling vegf-response of purkinje cells by downregulation of kdr via mirna-204-5p. *Int J Mol Sci.* **22** (4), 2173 (2021).
34. Wolters, A. et al. Teriflunomide provides protective properties after oxygen-glucose-deprivation in hippocampal and cerebellar slice cultures. *Neural Regen Res.* **16** (11), 2243-2249 (2021).
35. Gorter, R. P., Dijksman, N. S., Baron, W., Colognato, H. Investigating demyelination, efficient remyelination and remyelination failure in organotypic cerebellar slice cultures: Workflow and practical tips. *Methods Cell Biol.* **168**, 103-123 (2022).
36. Lamoureux, L. et al. Non-productive infection of glial cells with sars-cov-2 in hamster organotypic cerebellar slice cultures. *Viruses.* **14** (6), 1218 (2022).

37. Frontzek, K. et al. A conformational switch controlling the toxicity of the prion protein. *Nat Struct Mol Biol.* **29** (8), 831-840 (2022).

38. Tellios, V., Maksoud, M. J. E., Nagra, R., Jassal, G., Lu, W. Y. Neuronal nitric oxide synthase critically regulates the endocannabinoid pathway in the murine cerebellum during development. *Cerebellum.* **22** (6), 1200-1215 (2023).

39. Schroder, L. J. et al. Polysialic acid promotes remyelination in cerebellar slice cultures by siglec-e-dependent modulation of microglia polarization. *Front Cell Neurosci.* **17**, 1207540 (2023).

40. Tzur-Gilat, A., Ziv, Y., Mittelman, L., Barzilai, A., Shiloh, Y. Studying the cerebellar DNA damage response in the tissue culture dish. *Mech Ageing Dev.* **134** (10), 496-505 (2013).

41. Tal, E. et al. Inactive atm abrogates dsb repair in mouse cerebellum more than does atm loss, without causing a neurological phenotype. *DNA Repair (Amst).* **72**, 10-17 (2018).

42. Tal, E. Shiloh, Y. Monitoring the atm-mediated DNA damage response in the cerebellum using organotypic cultures. *Methods Mol Biol.* **1599**, 419-430 (2017).

43. Dar, I. et al. Investigation of the functional link between atm and nbs1 in the DNA damage response in the mouse cerebellum. *J Biol Chem.* **286** (17), 15361-15376 (2011).

44. Barlow, C. et al. Atm-deficient mice: A paradigm of ataxia telangiectasia. *Cell.* **86** (1), 159-171 (1996).

45. Elson, A. et al. Pleiotropic defects in ataxia-telangiectasia protein-deficient mice. *Proc Natl Acad Sci U S A.* **93** (23), 13084-13089 (1996).

46. Xu, Y. et al. Targeted disruption of atm leads to growth retardation, chromosomal fragmentation during meiosis, immune defects, and thymic lymphoma. *Genes Dev.* **10** (19), 2411-2422 (1996).

47. Borghesani, P. R. et al. Abnormal development of purkinje cells and lymphocytes in atm mutant mice. *Proc Natl Acad Sci U S A.* **97** (7), 3336-3341 (2000).

48. Rahmanian, N., Shokrzadeh, M., Eskandani, M. Recent advances in gammah2ax biomarker-based genotoxicity assays: A marker of DNA damage and repair. *DNA Repair (Amst).* **108**, 103243 (2021).

49. Furia, L., Pelicci, S., Scanarini, M., Pelicci, P. G., Faretta, M. From double-strand break recognition to cell-cycle checkpoint activation: High content and resolution image cytometry unmasks 53bp1 multiple roles in DNA damage response and p53 action. *Int J Mol Sci.* **23** (17), 10193 (2022).

50. Duma, L. Ahel, I. The function and regulation of adp-ribosylation in the DNA damage response. *Biochem Soc Trans.* **51** (3), 995-1008 (2023).

51. Komulainen, E. et al. Parp1 hyperactivity couples DNA breaks to aberrant neuronal calcium signalling and lethal seizures. *EMBO Rep.* **22** (5), e51851 (2021).

52. Hendelman, W. J. Aggerwal, A. S. The purkinje neuron: I. A golgi study of its development in the mouse and in culture. *J Comp Neurol.* **193** (4), 1063-1079 (1980).

53. Aggerwal, A. S. Hendelman, W. J. The purkinje neuron: Ii. Electron microscopic analysis of the mature purkinje neuron in organotypic culture. *J Comp Neurol.* **193** (4), 1081-1096 (1980).

54. Hendelman, W. J., Jande, S. S., Lawson, D. E. Calcium-binding protein immunocytochemistry in organotypic

cultures of cerebellum. *Brain Res Bull.* **13** (1), 181-184 (1984).

55. Seil, F. J., Herndon, R. M., Tiekotter, K. L., Blank, N. K. Reorganization of organotypic cultures of mouse cerebellum exposed to cytosine arabinoside: A timed ultrastructural study. *J Comp Neurol.* **313** (2), 193-212 (1991).

56. Tauer, U., Volk, B., Heimrich, B. Differentiation of purkinje cells in cerebellar slice cultures: An immunocytochemical and golgi em study. *Neuropathol Appl Neurobiol.* **22** (4), 361-369 (1996).

57. Kapfhammer, J. P. Gugger, O. S. The analysis of purkinje cell dendritic morphology in organotypic slice cultures. *J Vis Exp.* (61), 3637 (2012).

58. Sherkhane, P. Kapfhammer, J. P. The plasma membrane ca2+-atpase2 (pmca2) is involved in the regulation of purkinje cell dendritic growth in cerebellar organotypic slice cultures. *Neural Plast.* **2013**, 321685 (2013).

59. Sherkhane, P. Kapfhammer, J. P. Chronic pharmacological blockade of the na(+) /ca(2+) exchanger modulates the growth and development of the purkinje cell dendritic arbor in mouse cerebellar slice cultures. *Eur J Neurosci.* **46** (5), 2108-2120 (2017).